Inorganic Chemistry

Article

pubs.acs.org/IC

Blue-Emitting $K_2Al_2B_2O_7:Eu^{2+}$ Phosphor with High Thermal Stability and High Color Purity for Near-UV-Pumped White Light-Emitting Diodes

Wenge Xiao,[†,‡] Xia Zhang,[†] Zhendong Hao,[†] Guo-Hui Pan,[†] Yongshi Luo,[†] Ligong Zhang,[†] and Jiahua Zhang*[,†]

[†]State Key Laboratory of Luminescence and Applications, Changchun Institute of Optics, Fine Mechanics and Physics, Chinese Academy of Sciences, Changchun 130033, China

[‡]University of Chinese Academy of Sciences, Beijing 100049, China

Supporting Information

ABSTRACT: Novel blue-emitting $K_2Al_2B_2O_7:Eu^{2+}$ ($KAB:Eu^{2+}$) phosphor was synthesized by solid state reaction. The crystal structural and photoluminescence (PL) properties of $KAB:Eu^{2+}$ phosphor, as well as its thermal properties of the photoluminescence, were investigated. The $KAB:Eu^{2+}$ phosphor exhibits broad excitation spectra ranging from 230 to 420 nm, and an intense asymmetric blue emission band centered at 450 nm under λ_{ex} = 325 nm. Two different Eu^{2+} emission centers in $KAB:Eu^{2+}$ phosphor were confirmed via their fluorescence decay lifetimes. The optimal concentration of Eu^{2+} ions in $K_{2-x}Eu_xAl_2B_2O_7$ was determined to be x = 0.04 (2 mol %), and the corresponding concentration quenching mechanism was verified to be the electric dipole−dipole interactions. The PL intensity of the nonoptimized $KAB:0.04Eu^{2+}$ phosphor was measured to be ~58% that of the commercial blue-emitting $BaMgAl_{10}O_{17}:Eu^{2+}$ phosphor, and this phosphor has high color purity with the CIE coordinate (0.147, 0.051). When heated up to 150 °C, the $KAB:0.04Eu^{2+}$ phosphor still has 82% of the initial PL intensity at room temperature, indicating its high thermal stability. These results suggest that the $KAB:Eu^{2+}$ is a promising candidate as a blue-emitting n-UV convertible phosphor for application in white light emitting diodes.

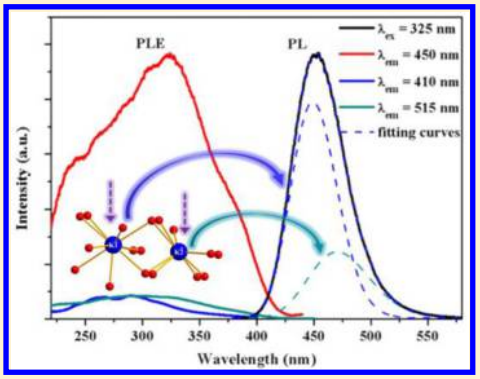

1. INTRODUCTION

Recently, white light emitting diodes (w-LEDs) made from blue or near-ultraviolet (n-UV) LEDs coated with phosphors have been attracting much attention for their high luminous efficiency, low energy consumption, good durability, and safety.[1−3] Current commercial w-LEDs are fabricated by the combination of blue-emitting InGaN LEDs and yellow-emitting $Y_3Al_5O_{12}:Ce^{3+}$ ($YAG:Ce^{3+}$) phosphor. However, this method suffers from high correlated color temperature (CCT > 4500 K) and poor color-rendering index (Ra < 80) due to the deficiency of red emission in the visible region, which largely restrain its application to general lighting.[4−9] An alternative method of combining n-UV LEDs (350−420 nm) with a mixture of red-, green-, and blue-emitting phosphors has been proposed and intensively studied.[10−14] This method can produce higher CRI values and better color stability due to the invisibility of n-UV light to the naked eye and smoother spectral distribution over the whole visible range. The eventual performance of the w-LEDs based on trichromatic phosphors strongly depends on the luminescence properties of the phosphors. Therefore, it is highly desirable to find new phosphors with high efficiency and good thermal stability which can be excited by n-UV LEDs.[15−19]

One of the highly efficient activators, Eu^{2+} ions, has broad emission and absorption spectra due to the allowed $5d-4f$ transitions between the $4f^7$ ground states and the $4f^65d^1$ excited states. Because the $5d$ energy levels of the Eu^{2+} ions are sensitive to the crystal field and covalency, it is possible to design a phosphor with special emission color by exploring a suitable compound to accommodate Eu^{2+} ions.[20,21] Accordingly, various Eu^{2+} ions doped phosphors for w-LEDs have been developed, such as the blue phosphors $KSrPO_4:Eu^{2+}$,[22] $Sr_4OCl_6:Eu^{2+}$,[23] $Ca_2PO_4Cl:Eu^{2+}$,[24] the green or yellow phosphors β-$SiAlON:Eu^{2+}$,[25] $Ba_{0.93}Eu_{0.07}Al_2O_4$,[26] $(Ca,Sr)_7(SiO_3)_6Cl_2:Eu^{2+}$,[27] and the red phosphors $(Ca_{1-x}Sr_x)S:Eu^{2+}$,[28] $Sr_2Si_5N_8:Eu^{2+}$,[29] $Sr[LiAl_3N_4]:Eu^{2+}$.[30]

Rare earth ions doped borate compounds as the luminescence materials have been widely investigated, as a result of their low synthetic temperature and good physical and chemical stability.[31−35] As for the potassium aluminum borate $K_2Al_2B_2O_7$ (KAB), the powder of KAB was preliminarily studied by Kaduk and Satek at first, and then the crystal of KAB was found to be a new UV nonlinear optical crystal.[36,37] Therefore, the crystal growth of KAB and its detail structure

Received: November 18, 2014
Published: March 9, 2015

DOI: 10.1021/ic502773t
Inorg. Chem. 2015, 54, 3189−3195

were intensively studied due to its easy crystal growth, good chemical stability, and mechanical properties and high UV transparency.[36−40] Recently, the optical properties of Dy^{3+} doped KAB for n-UV excited w-LEDs were reported by Palaspagar et al.[41] To the best of our knowledge, the luminescence properties of Eu^{2+} doped KAB (KAB:Eu^{2+}) and its potential application in w-LEDs have not yet been reported in the literature.

In the present work, a series of blue-emitting phosphors, Eu^{2+} doped KAB, were synthesized by solid state reaction. And the structural and photoluminescence properties of KAB:Eu^{2+} were investigated in detail. The phosphor shows intense blue emission peaking at 450 nm under the excitation of the light of 230−420 nm that overlaps well with the electroluminescence of n-UV LEDs. Moreover, the KAB:Eu^{2+} phosphor exhibits good thermal stability and high color purity. Consequently, it is believed that this novel KAB:Eu^{2+} phosphor can act as a blue-emitting phosphor for n-UV excited w-LEDs.

2. EXPERIMENTAL SECTION

2.1. Materials and Synthesis. Powder phosphor samples with different concentrations of Eu^{2+} (0.5, 1, 2, 3, 4, and 5 mol %) doped $K_2Al_2B_2O_7$ were prepared by solid state reaction. In order to avoid the hygroscopic property of K_2CO_3 and reach better homogenization, the solution method was used before sintering. Typically, Eu_2O_3 (4N) was dissolved in HNO_3 (G.R.) to obtain $Eu(NO_3)_3$. Then the stoichiometric amounts of K_2CO_3 (A.R.), Al $(NO_3)_3$ (A.R.), H_3BO_3 (A.R.) and $Eu(NO_3)_3$ were mixed and continuously stirred for 2 h, and subsequently heated in an oven at 85 °C until the solvent dried up completely, then heated at 150 °C for 8 h to remove the crystal water. After being ground for 5 min in an agate mortar, the mixtures were preheated at 550 °C for 2 h, and then sintered at 1000 °C for 8 h in a CO reducing atmosphere by burying the crucibles in spectrum pure carbon sticks.

2.2. Characterization. The powder X-ray diffraction (XRD) patterns were collected on a Bruker D8 Focus diffractometer, in the 2θ range from 15° to 70° with Cu Kα radiation (λ = 1.54056 Å) operated at 40 kV and 40 mA. The measurements of the photoluminescence (PL), photoluminescence excitation (PLE) and diffuse reflectance (DR) spectra were performed with a Hitachi F-7000 spectrometer equipped with a 150 W xenon lamp as the excitation source. White $BaSO_4$ (reflection 100%) was used as the standard reference for reflection measurement. And for comparison, commercial blue-emitting $BaMgAl_{10}O_{17}$:Eu^{2+} (BAM:Eu^{2+}) phosphor was used as the state-of-the-art reference. And the temperature-dependent PL spectra were also carried out on F-7000 spectrometer with an external heater. A process controller (OMEGA CN76000) equipped with a thermocouple was used to measure the temperature and control the heating rate. In fluorescence lifetime measurements, an optical parametric oscillator (OPO) was used as an excitation source and the signal was detected by a Tektronix digital oscilloscope (TDS 3052). All the measurements were conducted at room temperature unless mentioned specially.

3. RESULTS AND DISCUSSION

3.1. Structural Properties of the KAB:Eu^{2+} Phosphor. The purities of the as-prepared samples were examined by XRD. Figure 1 shows the XRD patterns of undoped and 2 mol % Eu^{2+} doped KAB samples. From Figure 1, we can see that all

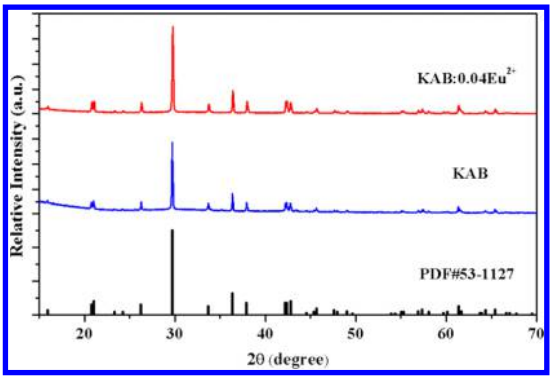

Figure 1. XRD patterns of the as-synthesized KAB and KAB:0.04Eu^{2+}.

the diffraction peaks agree well with that of the JCPDS standard pattern (PDF#53-1127). This indicates that the single phase KAB powder was obtained in our study, and Eu^{2+} ions can be completely dissolved in the host lattice without generating any impurity phase. KAB crystallizes in a trigonal system with space group *P*321 and with three chemical formula units per unit cell. The dimensions of the unit cell are $a = b = 8.530$ Å, $c = 8.409$ Å, and $V = 829.9$ Å^3.[36] As depicted in Figure 2a, the basic structural features of the KAB crystal include K^+ ions, $(BO_3)^{3-}$ groups, and $(AlO_4)^{5-}$ groups. The two latter groups form an approximately planar $(Al_3B_3O_6)$ network with all the $(BO_3)^{3-}$

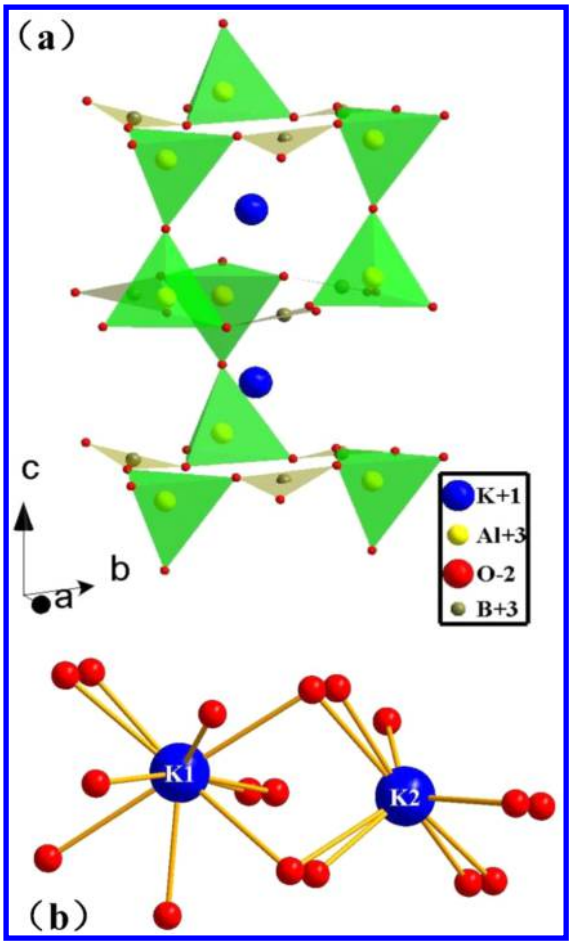

Figure 2. (a) Crystal structure of KAB in a trigonal system with space group *P*321; (b) Two different potassium sites are depicted with nine- and ten-coordination oxygen atoms.

DOI: 10.1021/ic502773t
Inorg. Chem. 2015, 54, 3189−3195

groups perpendicular to the *c* axis, and the layers are bridged by oxygen atoms, which are bounded to the Al atoms of adjacent layers. The K^+ ions are arranged in the interstices formed by the adjacent layers. Two different crystallographic positions are available for K^+ ions. One is the Wyckoff symbol 3e site coordinated by ten oxygen atoms, and the other is the 3f site coordinated by nine oxygen atoms, denoted as K1 and K2, respectively (see Figure 2b).[37,39,40] As regards KAB:xEu^{2+}, it is assumed that Eu^{2+}(r = 1.30 Å when coordination number (CN) = 9 and r = 1.35 Å when CN = 10) ions can randomly enter the two different K^+ (r = 1.55 Å when CN = 9 and r = 1.59 Å when CN = 10) sites because both the Al^{3+} (r = 0.39 Å when CN = 4) and the B^{3+}(r = 0.01 Å when CN = 3) sites are too small to be occupied.[42] Accordingly, two different emission centers, originating from the different sites, will be formed.

3.2. Photoluminescence Properties. The PLE and PL spectra of the sample KAB:0.04Eu^{2+} are shown in Figure 3.

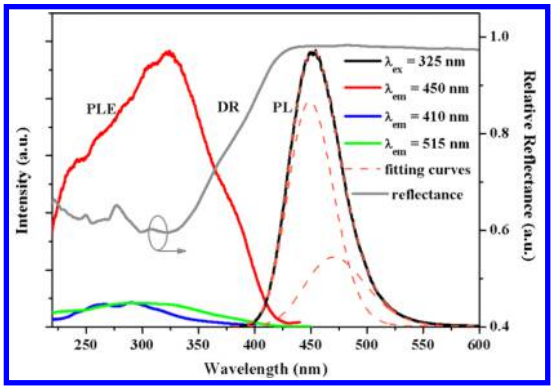

Figure 3. PLE, PL, and the relative DR spectra of KAB:0.04Eu^{2+} and the decomposed PL spectra with the peak wavelengths of 447 and 470 nm, respectively.

Under the excitation of 325 nm UV radiation, the sample exhibits a strong and asymmetric blue emission which extends from 400 to 550 nm centered at 450 nm, ascribed to the allowed electronic transition of $4f^65d^1$ to $4f^7$ of Eu^{2+} ions. And the PLE spectra (monitored at 450 nm) consists of a broad unresolved band ranging from 230 to 420 nm which is attributed to the direct excitation from the $4f^7$ to $4f^65d^1$ of Eu^{2+} ions, indicating its potential application in n-UV pumped w-LEDs. The relative DR spectra (see Figure 3) of Eu^{2+} doped KAB compared to the undoped sample confirm that the absorption of this phosphor in the region from 230 to 420 nm can be mainly ascribed to the allowed $5d$–$4f$ transitions of Eu^{2+} ions (the DR spectra of undoped and Eu^{2+} doped KAB samples were shown in Figure S1). The asymmetry of PL spectra and the broadness of PLE spectra of the KAB:Eu^{2+} demonstrate the presence of different emission centers due to the existence of two potassium crystallographic sites which can provide two sites for Eu^{2+} ions to accommodate, as discussed above. Decomposition of the PL spectra can be used to identify the presence of two emission bands of the Eu^{2+} ions. Hence, the PL spectra of KAB:Eu^{2+} were decomposed using two Gaussian equations with the peak wavelengths of 447 and 470 nm, respectively. More details about the decomposition of the PL spectra on the energy scale are available in Figure S2 and S3. Moreover, in order to avoid mutual interference in two emission centers, we obtained the PLE spectra while monitoring at 410 and 515 nm, respectively. Obviously, the PLE spectra have different shapes, as shown in Figure 3, which may also result from the different site occupancy of Eu^{2+} ions. In order to confirm the existence of two different Eu^{2+} emission centers, the decay curves of the two emissions of KAB:0.04Eu^{2+} under pulse laser excitation at 355 nm were measured and plotted in Figure 4. Obviously, the two decay curves show the

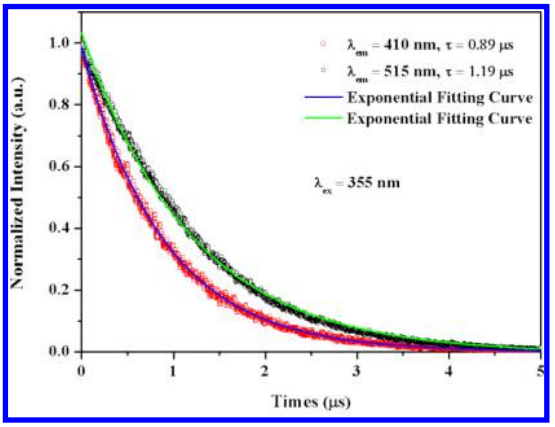

Figure 4. Experimental data and single exponential fitting curves of the time-resolved emission of KAB:0.04Eu^{2+} under pulse laser excitation at 355 nm.

different lifetimes and each decay curve can be well fitted with a single exponential function with the lifetime of 0.89 μs for the Eu^{2+} center located at the shorter wavelength and 1.19 μs for the Eu^{2+} center located at the longer wavelength.

To further understand the origin of the two emission bands of Eu^{2+} ions, a well-known empirical equation given by Van Uitert has been used.[23] According to his discussion, the emission position of the Eu^{2+} ions is strongly dependent on its local environment and obeys an empirical relation between the energetic position of the Eu^{2+} emission and the local structure in various compounds. The relation was given as[43]

$$E = Q\left[1 - \left(\frac{V}{4}\right)^{1/V} \times 10^{-n\times EA\times r/80}\right] \quad (1)$$

where E is the position of the PL band of Eu^{2+} (cm^{-1}), Q is the position in energy for the lower d-band edge of the free Eu^{2+} ion (Q = 34000 cm^{-1}), V is the valence state of the Eu^{2+} ions (V = 2), n relates to the number of anions in the immediate shell of the Eu^{2+} ion, which is the coordination number of Eu^{2+}, EA is the electron affinity of the anions around the Eu^{2+} ions (eV), and r is the ionic radius of the host cation replaced by Eu^{2+}. It is hard to calculate precisely the exact energy levels of Eu^{2+} at a specific site through this formula because of the complexity of the local structure. But we can readily deduce that the value of E is proportional to the quantity of n and r. On the basis of the above effective ionic radii of K^+, we conclude that the band peaked at 447 nm can be attributed to the $4f^65d^1 \rightarrow 4f^7$ transition of Eu^{2+} ions occupying the K1 sites with ten-coordination, while the longer wavelength band is attributed to Eu^{2+} ions occupying K2 sites with nine-coordination.

The concentration dependence of the PL intensity of the samples KAB:xEu^{2+} with x = 0.01, 0.02, 0.04, 0.06, 0.08, and 0.1, was depicted in Figure 5. With increasing the Eu^{2+} concentration, the PL intensity of KAB:xEu^{2+} increases first and reaches a maxima; then the intensity tends to decrease gradually due to the concentration quenching effect. The optimal doping concentration of Eu^{2+} ions was determined to

DOI: 10.1021/ic502773t
Inorg. Chem. 2015, 54, 3189–3195

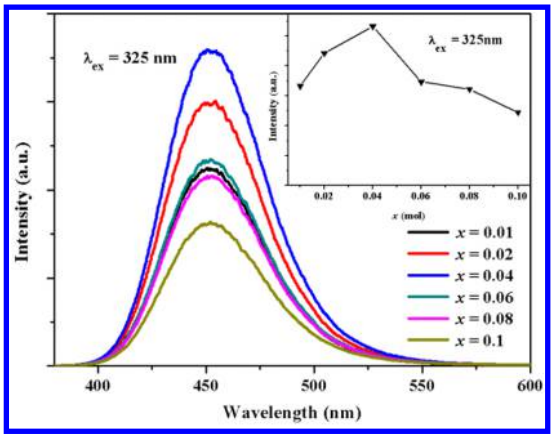

Figure 5. PL spectra of KAB:xEu^{2+}(x = 0.01−0.1) under the excitation of 325 nm. The inset shows the dependence of the integrating intensity on the concentration of Eu^{2+} ions.

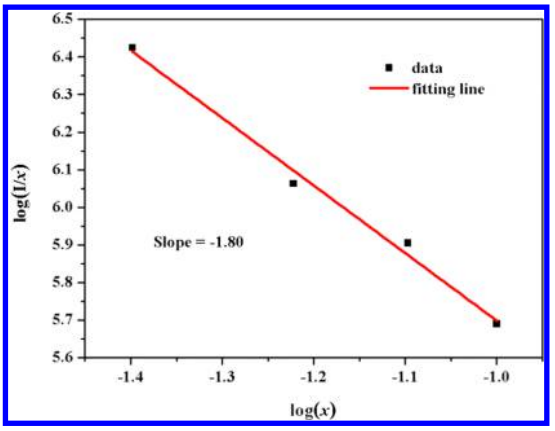

Figure 6. Linear fitting of log(x) versus log(I/x) in the KAB:xEu^{2+} samples.

be 0.04, beyond which the concentration quenching effect will dominate over the increase of activator centers. The concentration quenching originates from the larger probability of energy loss at a killer center due to excitation energy migration among activators at higher concentration. As proposed by Blasse, the critical energy transfer distance (R_c), defined as the distance for which the probability of energy transfer equals the probability of radiative transition of the activator ions, can be estimated from geometrical consideration by the following formula:[44]

$$R_c \approx 2\left[\frac{3V}{4\pi X_c N}\right]^{1/3} \quad (2)$$

where V represents the volume of the unit cell, X_c represents the critical concentration of Eu^{2+} ions, and N represents the number of total Eu^{2+} sites in the unit cell. In this case, V = 829.9 Å^3, N = 6, and X_c = 0.04. Thus, the R_c of Eu^{2+} ions was calculated to be 18.7 Å. It is known that the energy transfer mechanism includes radiation reabsorption, exchange coupling, or electric multipolar interactions, since the mechanism of radiation reabsorption is only effective when the fluorescence spectra are broadly overlapping, and the exchange coupling takes place generally in a forbidden transition (the R_c is typically ∼5 Å). Thus, both of them play a negligible role for the energy migration between Eu^{2+} ions in the KAB:Eu^{2+} phosphor. Therefore, the energy transfer mechanism among Eu^{2+} ions in this system is governed by electric multipolar interactions based on the Dexter theory. Furthermore, according to the report of Van Uitert the PL intensity per activator concentration can be calculated by the following equation:[45,46]

$$\frac{I}{x} = \frac{k}{1 + \beta(x)^{\theta/3}} \quad (3)$$

where I is the PL intensity, x is the activator ion concentration, which is not less than the critical concentration, k and β are constants for a given host crystal under the same excitation conditions, and θ is an indication of the type of electric multipolar interactions. The value of θ is 6, 8, and 10, standing for the energy transfer mechanism of electric dipole−dipole, dipole−quadrupole, and quadrupole−quadrupole interactions, respectively. As shown in Figure 6, the relationship of log(I/x) versus log(x) can be fitted linearly with a slope $-(\theta/3)$ equal to −1.8. The value of θ was determined to be 5.4, which approximates to 6, implying that the concentration quenching of Eu^{2+} ions in the KAB:Eu^{2+} mainly results from the electric dipole−dipole interactions. With the assumption that energy transfer between Eu^{2+} occurs mainly via the electric dipole−dipole interactions, Dexter figured out an alternative critical distance R_c calculation method, given as[47]

$$R_c^6 = 0.63 \times 10^{28} \frac{(4.8 \times 10^{-16})P}{E^4} \int f_s(E)F_a(E)dE \quad (4)$$

where $4.8 \times 10^{-16}P$ is the absorption coefficient of Eu^{2+}, P is the oscillator strength of the transition, which is taken as 0.01 for Eu^{2+}, E (in eV) is the energy of maximum spectral overlap, and $\int f_s(E)F_a(E)dE$ represents the spectral overlap integral from the normalized PLE and PL spectra of KAB:Eu^{2+}. From the experimental spectral data, E and $\int f_s(E)F_a(E)dE$ were calculated to be 3.04 and 0.027 eV^{-1}; therefore, the value of R_c derived from the spectral data is about 14.6 Å, which is in good consistency with Blasse's method. This result further confirms that the energy transfer between Eu^{2+} ions arises from the electric dipole−dipole interactions.

3.3. Temperature-Dependent Photoluminescence and Potential Application for w-LEDs. For the application of w-LEDs, especially the high-power one, the thermal stability of the phosphor should be considered. Temperature-dependent PL spectra of KAB:0.04Eu^{2+} under the excitation of 325 nm were investigated and are shown in Figure 7. As can be seen in the inset, the PL intensity of KAB:0.04Eu^{2+} drops to 82% when the temperature is raised up to 150 °C. Compared with the commercial phosphors and the reported phosphors with excellent performance in Table S1, KAB:0.04Eu^{2+} has a relatively high thermal stability upon heating. And the full widths at half-maximum (FWHMs) of the PL spectra of KAB:0.04Eu^{2+} increase from 53 to 60 nm. These phenomena can be explained by a physical model, known as a configuration coordinate diagram, that when temperature increases, electron−phonon interaction is enhanced and the population of higher vibration levels is increased. With the help of phonons, the excited luminescent center is thermally activated and subsequently released nonradiatively through the crossover between the excited states and the ground states. As a result, the luminescence is quenched due to enhanced population density of phonons, which also causes the broadening of the PL spectra.[48,49] Besides, the emission band is a little blue-shifted with raising the temperature. And similar blue-shifts were also

DOI: 10.1021/ic502773t
Inorg. Chem. 2015, 54, 3189−3195

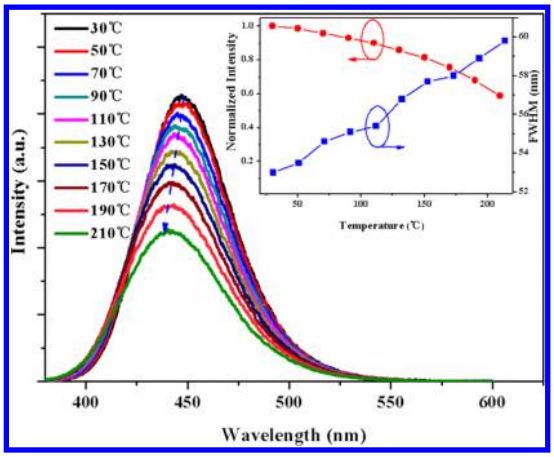

Figure 7. Temperature-dependent PL spectra of KAB:0.04Eu^{2+} excited at 325 nm. The inset shows the normalized PL intensity and the FWHMs as a function of temperature.

observed elsewhere, such as Ca_2SiO_4:Eu^{2+}, Ba_2SiO_4:Eu^{2+} and Sr_3SiO_5:Eu^{2+}.[48−50] It was ascribed to the thermally active phonon-assisted tunnelling from the excited states of the low-energy emission band to the excited states of the high-energy emission band in the configuration coordinate diagram. As discussed before, there are two emission centers for the KAB:Eu^{2+} phosphor. At higher temperature, the thermal back-transfer from lower energy centers to higher energy centers is more possible; consequently, the higher energy emission is strengthened. Thus, the blue-shift phenomenon is observed with the increase of temperature. In addition, it is also possible that the host lattice is expanded as the temperature increases, which would cause a reduction in the crystal field splitting and lead to a higher energy emission.

To better understand the temperature dependence of photoluminescence, the activation energy was calculated using the Arrhenius equation given as[18,23]

$$I(T) = \frac{I_0}{1 + A \cdot e^{(-E_a/k_B T)}} \quad (5)$$

where I_0 is the initial PL intensity of the phosphor at room temperature, $I(T)$ is the PL intensity at a given temperature T, A is a constant, E_a is the activation energy for thermal quenching, and k_B is the Boltzmann constant (8.617×10^{-5} eV K^{-1}). Figure 8 depicts a plot of $\ln[(I_0/I) - 1]$ versus $1/(k_B T)$. Through the best fit using the Arrhenius equation, E_a was obtained to be 0.30 eV for KAB:Eu^{2+}. The relatively high activation energy indicates good thermal stability for this phosphor, which is an essential condition for practical application.

Furthermore, the comparison of the PLE and PL spectra between the blue KAB:Eu^{2+} phosphor and the commercial one BAM:Eu^{2+} is show in Figure 9b. When excited at 325 nm, the integrated area of the PL spectra was measured to be ∼58% that of the commercial blue BAM:Eu^{2+} phosphor, although KAB:Eu^{2+} is yet to be fully optimized. As key parameters, the CIE coordinates for the KAB:Eu^{2+} sample excited at 365 nm were determined to be (0.147, 0.051), indicating that this phosphor has a high color purity as shown in Figure 9b. A digital photograph of sample under 365 nm UV lamps is shown in the inset, revealing an intense blue emission. The initial results suggest that this novel phosphor may serve as a promising candidate for w-LEDs application.

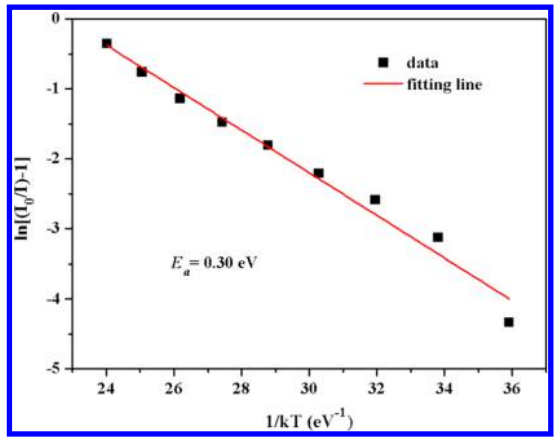

Figure 8. Fitted activation energy for thermal quenching of KAB:0.04Eu^{2+} using the Arrhenius equation.

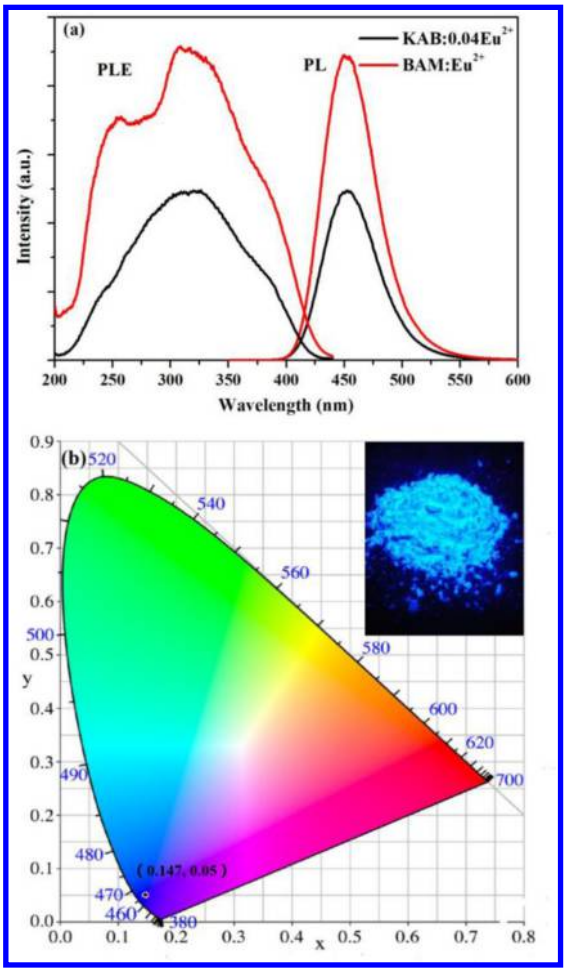

Figure 9. (a) Comparison of PLE (λ_{em} = 450 nm) and PL (λ_{ex} = 325 nm) spectra of KAB:Eu^{2+} with that of commercial blue BAM:Eu^{2+} phosphor; (b) CIE coordinate of the KAB:Eu^{2+} phosphor. The inset shows the image of the KAB:Eu^{2+} phosphor under 365 nm UV lamps.

4. CONCLUSION

In conclusion, a new blue-emitting phosphor, KAB:Eu^{2+}, was synthesized by solid state reaction and the photoluminescence properties were studied in detail. The obtained KAB:Eu^{2+} phosphor shows bright blue emission centered at 450 nm under the excitation of light ranging from 230 to 420 nm, which matches well with the emission of n-UV LED chips. Two

DOI: 10.1021/ic502773t
Inorg. Chem. 2015, 54, 3189−3195

different emissions peaking at 447 and 470 nm were observed for KAB:Eu^{2+}, originating from the presence of two different potassium sites in the KAB host, which was confirmed by their lifetimes evaluated to be 0.89 and 1.19 μs, respectively. The optimal concentration was determined to be 2 mol %, and the critical distance for Eu^{2+} ions in KAB: Eu^{2+} was calculated to be 18.7 and 14.6 Å using two methods proposed by Blasse and Dexter, respectively, which verified that the energy transfer between Eu^{2+} ions occurs through the electric dipole−dipole interactions. The temperature dependence of the photoluminescence demonstrates that the PL intensity of KAB:0.04Eu^{2+} retains 82% when the temperature is raised up to 150 °C, and the activation energy was calculated to be 0.30 eV using the Arrhenius equation, indicating its high thermal stability. With temperature increasing, the emission band is blue-shifted slightly, which was explained in terms of the thermally active phonon-assisted tunnelling from the excited states of the low-energy emission band to the excited states of the high-energy emission band in the configuration coordinate diagram. The PL intensity of the as-synthesized KAB:Eu^{2+} sample achieves ∼58% that of the commercial blue BAM:Eu^{2+} phosphor under the excitation of 325 nm. Finally, the CIE coordinates were measured as (0.147, 0.051), indicating its high color purity. As discussed, the developed KAB:Eu^{2+} phosphor is a potential blue-emitting component for n-UV excited w-LEDs.

■ ASSOCIATED CONTENT

Ⓢ Supporting Information

DR spectra of the undoped and Eu^{2+} doped sample, Gaussian decomposition of the PL spectra on the energy scale, and a table giving the temperature characteristic of some reported phosphors with excellent performance. This material is available free of charge via the Internet at http://pubs.acs.org.

■ AUTHOR INFORMATION

Corresponding Author

* E-mail: zhangjh@ciomp.ac.cn. Tel.: +86-431-86176317 Fax.: +86-431-86176317.

Notes

The authors declare no competing financial interest.

■ ACKNOWLEDGMENTS

This work is financially supported by the National Natural Science Foundation of China (51172226, 61275055, 11274007 and 11174278) and the Natural Science Foundation of Jilin province (201205024, 20140101169JC).

■ REFERENCES

(1) Pimputkar, S.; Speck, J. S.; Denbaars, S. P.; Nakamura, S. *Nat. Photonics* **2009**, *3*, 2−4.
(2) Chen, L.; Lin, C.-C.; Yeh, C.-W.; Liu, R.-S. *Materials* **2010**, *3*, 2172−2195.
(3) Shang, M.; Li, C.; Lin, J. *Chem. Soc. Rev.* **2014**, *43*, 1372−1386.
(4) Hye Oh, J.; Ji Yang, S.; Rag Do, Y. *Light: Sci. Appl.* **2014**, *3*, e141.
(5) Setlur, A. A.; Heward, W. J.; Hannah, M. E.; Happek, U. *Chem. Mater.* **2008**, *20*, 6277−6283.
(6) Setlur, A. A.; Heward, W. J.; Gao, Y.; Srivastava, A. M.; Chandran, R. G.; Shankar, M. V. *Chem. Mater.* **2006**, *2*, 3314−3322.
(7) Wang, L.; Zhang, X.; Hao, Z.; Luo, Y.; Wang, X.; Zhang, J. *Opt. Express* **2010**, *18*, 25177−25182.
(8) Lü, W.; Lv, W.; Zhao, Q.; Jiao, M.; Shao, B.; You, H. *Inorg. Chem.* **2014**, *53*, 11985−11990.
(9) Lee, S. P.; Huang, C. H.; Chan, T. S.; Chen, T. M. *ACS Appl. Mater. Interfaces* **2014**, *6*, 7260−7267.
(10) Lü, W.; Guo, N.; Jia, Y.; Zhao, Q.; Lv, W.; Jiao, M.; You, H. *Inorg. Chem.* **2013**, *52*, 3007−3012.
(11) Nishida, T.; Ban, T.; Kobayashi, N. *Appl. Phys. Lett.* **2003**, *82*, 3817−3819.
(12) Yu, J.; Hao, Z.; Zhang, X.; Luo, Y.; Zhang, J. *Chem. Commun.* **2011**, *47*, 12376−12378.
(13) Sheu, J.; Chang, S.; Kuo, C.; Su, Y.; Wu, L.; Lin, Y.; Lai, W.; Tsai, J.; Chi, G.; Wu, R. *IEEE Photon. Technol. Lett.* **2003**, *15*, 18−20.
(14) Radkov, E.; Bompiedi, R.; Srivastava, A. M.; Setlur, A.; Becker, C. *Proc. SPIE* **2004**, *5187*, 171−177.
(15) Li, K.; Geng, D.; Shang, M.; Zhang, Y.; Lian, H.; Lin, J. *J. Phys. Chem. C* **2014**, *118*, 11026−11034.
(16) Ji, H.; Huang, Z.; Xia, Z.; Molokeev, M. S.; Atuchin, V. V.; Fang, M.; Huang, S. *Inorg. Chem.* **2014**, *53*, 5129−5135.
(17) Wang, Z.; Zhang, Y.; Xiong, L.; Li, X.; Guo, J.; Gong, M. *Curr. Appl. Phys.* **2012**, *12*, 1084−1087.
(18) Wang, D.-Y.; Wu, Y.-C.; Chen, T.-M. *J. Mater. Chem.* **2011**, *21*, 18261−18265.
(19) Hao, Z.; Zhang, J.; Zhang, X.; Sun, X.; Luo, Y.; Lu, S.; Wang, X. *Appl. Phys. Lett.* **2007**, *90*, 261113.
(20) Weakliem, H. *Phys. Rev. B* **1964**, *6*, 2743−2748.
(21) Poort, S. H. M.; Blasse, G. *J. Lumin.* **1997**, *72*−*74*, 247−249.
(22) Tang, Y.-S.; Hu, S.-F.; Lin, C. C.; Bagkar, N. C.; Liu, R.-S. *Appl. Phys. Lett.* **2007**, *90*, 151108.
(23) Gwak, S. J.; Arunkumar, P.; Im, W. B. *J. Phys. Chem. C* **2014**, *118*, 2686−2692.
(24) Chiu, Y.-C.; Liu, W.-R.; Chang, C.-K.; Liao, C.-C.; Yeh, Y.-T.; Jang, S.-M.; Chen, T.-M. *J. Mater. Chem.* **2010**, *20*, 1755−1758.
(25) Hirosaki, N.; Xie, R.-J.; Kimoto, K.; Sekiguchi, T.; Yamamoto, Y.; Suehiro, T.; Mitomo, M. *Appl. Phys. Lett.* **2005**, *86*, 211905.
(26) Li, X.; Budai, J. D.; Liu, F.; Howe, J. Y.; Zhang, J.; Wang, X.-J.; Gu, Z.; Sun, C.; Meltzer, R. S.; Pan, Z. *Light: Sci. Appl.* **2013**, *2*, e50.
(27) Daicho, H.; Iwasaki, T.; Enomoto, K.; Sasaki, Y.; Maeno, Y.; Shinomiya, Y.; Aoyagi, S.; Nishibori, E.; Sakata, M.; Sawa, H.; et al. *Nat. Commun.* **2012**, *3*, 1132.
(28) Hu, Y.; Zhuang, W.; Ye, H.; Zhang, S.; Fang, Y.; Huang, X. *J. Lumin.* **2005**, *111*, 139−145.
(29) Piao, X.; Horikawa, T.; Hanzawa, H.; Machida, K. *Appl. Phys. Lett.* **2006**, *88*, 161908.
(30) Pust, P.; Weiler, V.; Hecht, C.; Tücks, A.; Wochnik, A. S.; Henß, A.; Wiechert, D.; Scheu, C.; Schmidt, P. J.; Schnick, W. *Nat. Mater.* **2014**, *13*, 891−896.
(31) Lin, H.; Liang, H.; Han, B.; Zhong, J.; Su, Q.; Dorenbos, P.; Birowosuto, M.; Zhang, G.; Fu, Y.; Wu, W. *Phys. Rev. B* **2007**, *76*, 035117.
(32) Sun, J.; Sun, Y.; Lai, J.; Xia, Z.; Du, H. *J. Lumin.* **2012**, *132*, 3048−3052.
(33) Denault, K. A.; Cheng, Z.; Brgoch, J.; DenBaars, S. P.; Seshadri, R. *J. Mater. Chem. C* **2013**, *1*, 7339−7345.
(34) Yu, R.; Zhong, S.; Xue, N.; Li, H.; Ma, H. *Dalton Trans.* **2014**, *43*, 10969−10976.
(35) Liu, W.-R.; Huang, C.-H.; Wu, C.-P.; Chiu, Y.-C.; Yeh, Y.-T.; Chen, T.-M. *J. Mater. Chem.* **2011**, *21*, 6869−6874.
(36) Ning, Ye.; Wenrong, Z.; Baichang, Wu; Chuangtian, C. *Proc. SPIE* **1998**, *3556*, 21−23.
(37) Hu, Z. G.; Higashiyama, T.; Yoshimura, M.; Yap, Y. K.; Mori, Y.; Sasaki, T. *Jpn. J. Appl. Phys.* **1998**, *37*, 1093−1094.
(38) Zhang, C.; Wang, J.; Cheng, X.; Hu, X.; Jiang, H.; Liu, Y.; Chen, C. *Opt. Mater.* **2003**, *23*, 357−362.
(39) Hu, X. B.; Wang, J. Y.; Zhang, C. Q.; Xu, X. G.; Loong, C.-K.; Grimsditch, M. *Appl. Phys. Lett.* **2004**, *85*, 2241.
(40) Atuchin, V. V.; Bazarov, B. G.; Grossman, V. G.; Molokeev, M. S.; Bazarova, Z. G. *Proc. SPIE* **2013**, *8772*, 87721O.
(41) Palaspagar, R. S.; Sonekar, R. P.; Omanwar, S. K. *AIP Conf. Proc.* **2013**, *807*, 807−808.
(42) Shannon, R. D. *Acta Crystallogr.* **1976**, *36*, 751−767.
(43) Van Uitert, L. G. *J. Lumin.* **1984**, *29*, 1−9.
(44) Blasse, G. *Phys. Lett.* **1968**, *28*, 444−445.
(45) Van Uitert, L. G. *J. Chem. Phys.* **1966**, *44*, 3514−3522.

DOI: 10.1021/ic502773t
Inorg. Chem. 2015, 54, 3189−3195

(46) Van Uitert, L. G. *J. Electrochem. Soc.* **1967**, *114*, 1048−1053.
(47) Dexter, D. L. *J. Chem. Phys.* **1953**, *21*, 836−850.
(48) Ci, Z.; Que, M.; Shi, Y.; Zhu, G.; Wang, Y. *Inorg. Chem.* **2014**, *53*, 2195−2199.
(49) Kim, J. S.; Park, Y. H.; Kim, S. M.; Choi, J. C.; Park, H. L. *Solid State Commun.* **2005**, *133*, 445−448.
(50) Baginskiy, I.; Liu, R. S.; Wang, C. L.; Lin, R. T.; Yao, Y. J. *J. Electrochem. Soc.* **2011**, *158*, P118−P121.

DOI: 10.1021/ic502773t
Inorg. Chem. 2015, 54, 3189−3195